Precision half-life measurement of ^{17}F

M. Brodeur,[1,*] C. Nicoloff,[1,2] T. Ahn,[1] J. Allen,[1] D. W. Bardayan,[1] F. D. Becchetti,[3] Y. K. Gupta,[1,4] M. R. Hall,[1] O. Hall,[1,5] J. Hu,[1,6] J. M. Kelly,[1] J. J. Kolata,[1] J. Long,[1] P. O'Malley,[1] and B. E. Schultz[1]

[1]*Department of Physics, University of Notre Dame, Notre Dame, Indiana 46556, USA*
[2]*Department of Physics, Wellesley College, Wellesley, Massachusetts 02481, USA*
[3]*Physics Department, University of Michigan, Ann Arbor, Michigan 48109, USA*
[4]*Nuclear Physics Division, Bhabha Atomic Research Centre, Mumbai 400085, India*
[5]*Department of Physics, University of Surrey, GU2 7XH, United Kingdom*
[6]*Institute of Modern Physics, Chinese Academy of Sciences, Lanzhou 730000, China*

(Received 8 December 2015; published 23 February 2016)

Background: The precise determination of ft values for superallowed mixed transitions between mirror nuclide are gaining attention as they could provide an avenue to test the theoretical corrections used to extract the V_{ud} matrix element from superallowed pure Fermi transitions. The ^{17}F decay is particularly interesting as it proceeds completely to the ground state of ^{17}O, removing the need for branching ratio measurements. The dominant uncertainty on the ft value of the ^{17}F mirror transition stems from a number of conflicting half-life measurements.

Purpose: A precision half-life measurement of ^{17}F was performed and compared to previous results.

Methods: The life-time was determined from the β counting of implanted ^{17}F on a Ta foil that was removed from the beam for counting. The ^{17}F beam was produced by transfers reaction and separated by the *TwinSol* facility of the Nuclear Science Laboratory of the University of Notre Dame.

Results: The measured value of $t_{1/2}^{\text{new}} = 64.402\,(42)$ s is in agreement with several past measurements and represents one of the most precise measurements to date. In anticipation of future measurements of the correlation parameters for the decay and using the new world average $t_{1/2}^{\text{world}} = 64.398\,(61)$ s, we present a new estimate of the mixing ratio ρ for the mixed transition as well as the correlation parameters based on assuming Standard Model validity.

Conclusions: The relative uncertainty on the new world average for the half-life is dominated by the large $\chi^2 = 31$ of the existing measurements. More precision measurements with different systematics are needed to remedy to the situation.

DOI: 10.1103/PhysRevC.93.025503

I. INTRODUCTION

In recent years, precision measurements have led to considerable advances in understanding nuclear astrophysics, nuclear structure, and fundamental symmetry [1,2]. With respect to the last topic, the combined efforts in improving the precision and accuracy of branching ratios, half-lives, and Q values of superallowed $0^+ \to 0^+$ pure Fermi β decays has led to the most stringent test of the unitarity of the Cabibbo–Kobayashi–Maskawa (CKM) matrix [3]. This, in turn, demonstrates the validity of the Standard Model (SM) for the electroweak interaction [4].

Indeed, the SM predicts that the CKM matrix, which relates the quarks' eigenstates under the weak interaction with their regular eigenstates, is unitary. A breakdown of unitarity could indicate new physics such as extra quark generations or exotic particles [5]. However, such a deviation should be approached with caution because erroneous data that shifted the value of V_{ud} have been found in the past [6]. The most precise unitarity test consists of summing the square of the top-row matrix elements: $|V_{ud}|^2 + |V_{us}|^2 + |V_{ub}|^2$. One of these critical elements in the unitarity test, V_{ud}, currently comes from 14 corrected $\mathcal{F}t$ values of superallowed $0^+ \to 0^+$ pure Fermi β decays [3]:

$$|V_{ud}|^2 = \frac{K}{\overline{\mathcal{F}t}\left(1+\Delta_R^V\right)G_F^2}, \tag{1}$$

where $K/(\hbar c)^6 = 2\pi^3\hbar \ln 2/(m_e c^2)^5 = 8120.2776\,(9) \times 10^{-10}\,\text{GeV}^{-4}$ s, G_F is the weak-interaction constant for the purely leptonic muon decay, Δ_R^V is the transition-independent part of the radiative correction, and $\overline{\mathcal{F}t}$ is the average of the 14 most precise $\mathcal{F}t$ values.

Despite the tremendous precision achieved in measurements of pure Fermi transitions, measurements in other systems, such as pion decays, neutron decays, and superallowed $0^+ \to 0^+$ mixed Fermi decays, could yield conflicting results that would point to unknown systematic effects or even new physics [7]. The mixed Fermi decays are particularly interesting because they can be used to test theoretical corrections used in evaluating pure Fermi decays. In particular, the extraction of the V_{ud} element from mirror transitions requires the measurement of an additional experimental quantity: the Fermi–Gamow–Teller mixing ratio ρ. This quantity can be calculated from three observables [7]: the β asymmetry parameter A_β, the neutrino asymmetry parameter B_ν, or the β-neutrino angular correlation coefficient $a_{\beta\nu}$. These are all inherently difficult to measure. Nevertheless, ρ is currently

*mbrodeur@nd.edu

known precisely for five mirror transitions: ^{19}Ne, ^{21}Na, ^{29}P, ^{35}Ar, and ^{37}K, and there are plans to measure it in more systems [8,9]. To make use of these future measurements however, it is necessary to improve the quality of the existing experimental data, which includes atomic masses, branching ratios, and half-lives.

Among the various mirror transitions, some of the most interesting cases are the lighter nuclides: ^{11}C, ^{13}N, ^{15}O, and ^{17}F. First, these transitions proceed completely from the ground state directly to the ground state of the daughter nuclei, which removes the often difficult task of measuring branching ratios [10]. Second, being low-mass nuclei, they could provide a complementary avenue to test for the presence of SM-forbidden scalar currents. However, the long half-lives of these nuclei make for challenging measurements of some of their correlation parameters [8]. Hence, with a shorter half-life of approximately 65 s, ^{17}F presents itself as an excellent first candidate. The lifetime of ^{17}F is currently known with less precision than the Q value, while being derived from a number of conflicting measurements resulting in a large Birge ratio of 2.8 [11,12]. Recently, the half-life of ^{17}F has been measured to a precision of 0.05% [12], disagreeing with three [13–15] of the past five measurements [13–17], including a lower-precision measurement [15] carried out by the same group. To help clarify the situation, an independent measurement of the ^{17}F half-life was performed at the Nuclear Science Laboratory of the University of Notre Dame.

II. EXPERIMENTAL METHOD

A radioactive ion beam of ^{17}F was produced from transfer reactions in inverse kinematics by using a ^{16}O beam passing through a deuterium gas target. The stable oxygen was produced by a source of negative ions from cesium sputtering (SNICS) and accelerated by an FN tandem with a terminal voltage of 8.1 MV. A mass-analyzing magnet downstream of the tandem was adjusted to select $^{16}O^{8+}$. After impinging on the gas target, the primary beam was stopped by a Faraday cup located at the entrance of the first superconducting magnet of the *TwinSol* facility [18], which refocused the reaction products past the exit of the magnet. A second solenoid was used to further separate $^{17}F^{8+}$ from the other reaction products. The solenoid magnetic field and the beam energy (set by the terminal voltage and the ion's charge state) were adjusted to maximize the ^{17}F-to-radioactive-contaminant ratio. The various nuclei present in the produced cocktail beam were monitored by using a ΔE-E silicon telescope. The particle identification plot for the optimal case (see Fig. 1) shows that a ^{17}F beam with minimal radioactive contamination exited the *TwinSol* facility. The only radioactive contamination identified in the particle identification plot was ^{15}O, in a ratio of $R = {}^{15}\mathrm{O}/{}^{17}\mathrm{F} = 2.4\,(6) \times 10^{-3}$. This is in contrast with the previous lifetime measurements of ^{17}F [14–16], which included larger contaminations that could make a half-life determination more difficult.

The ^{17}F lifetime was determined by using a technique where the ^{17}F ions were implanted in a thick tantalum foil (see Fig. 2). After a fixed time, the implanted foil was rotated

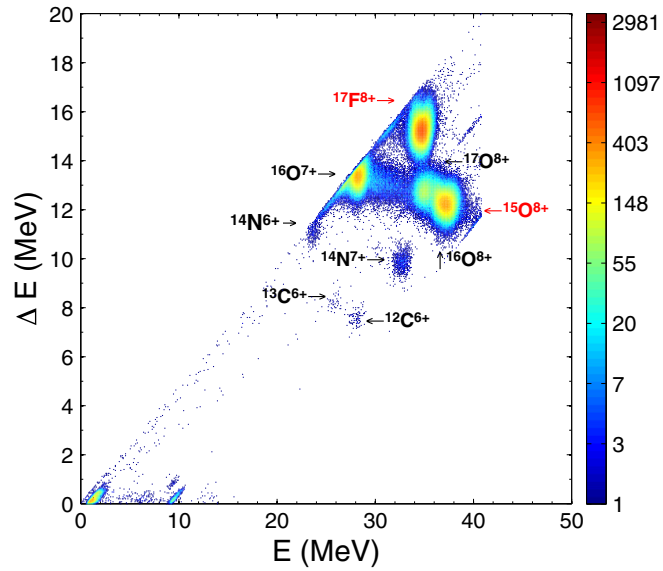

FIG. 1. Particle identification plot of the in coming cocktail beam separated by the *TwinSol* facility near the location of the β-counting station.

180° to face a 25-mm-thick plastic scintillator coupled to a photomultiplier tube. Signals were routed to a constant-fraction discriminator followed by a scaler. On the opposite end of the rotating arm, a second Ta foil, now placed in front of the beam, collected more radioactive samples while the counting of the first foil occurred. This simultaneous counting and irradiation made for efficient use of the beam. This switching process was repeated for N number of samples, creating what will be referred to as a run. The ensemble of all the runs formed the complete experiment. During the measurement, the scaler was referenced to an accurate (found to deviate by no more than 3 s over a period of 10 hours) 100 Hz clock, allowing each individual count to be time stamped with 10 ms precision. The data were saved in a list format with each count as an entry together with the real and live times provided by the

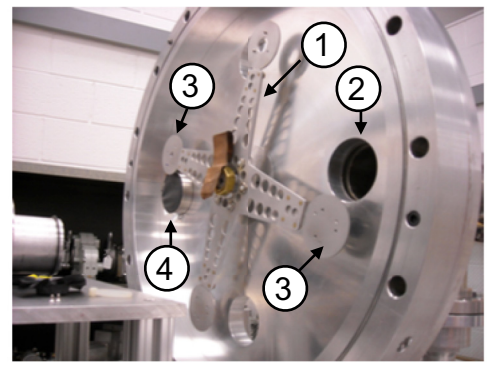

FIG. 2. The University of Notre Dame β-decay counting station. The station comprises (1) a rotatable arm, (2) a port from which the ion beam enters the station, (3) two foil holders used for the experiment, and (4) a plastic scintillator detector facing the implanted foil, and connected to a photomultiplier tube.

TABLE I. Characteristics of the three experimental runs. N_{samples} is the number of samples and N_{bins} is the number of bins for the given run.

Run	Duration (×65 s)	Bin size (ms)	N_{samples}	N_{bins}
1	8	40	70	13000
2	10	40	11	16250
3	20	80	18	16250

clock. After each event was triggered, a fast veto signal was generated that forced the system to be dead for 24.3 (2) μs, assuring that no arriving counts could trigger the scaler. This assured that the dead time per event was fixed [19] and hence count-rate and time independent.

III. DATA ANALYSIS

The data analysis essentially followed the well-established, widely used procedure outlined in Ref. [20]. Two separate programs were written and the data analysis was performed separately by two different group members. These programs were also tested against artificially created data to ensure their fitting accuracy. The analysis is presented in detail in the following section.

A. Data preselection

The data were first screened for samples with any abnormally low (<1000) total number of counts. It was discovered that all samples with low count numbers coincided with an incomplete sample where a run was prematurely terminated. During the experiment, the total number of detected counts per sample varied between 6.4×10^4 and 1.1×10^5. A total of three runs of different length were performed to investigate any possible systematic effect associated with varying the length of a sample. Table I outlines the characteristics of each run. Sample lengths of 8, 10, and 20 times 65 s, the approximate half-life of ^{17}F, were chosen. In the following analysis, the data have been rebinned from the original 13 000 and 16 250 bins down to 250 bins, a common number of bins used by other groups, to avoid having a large number of bins with zero counts. Such empty bins could introduce a bias into the fitting procedure.

B. Half-life determination

The data were fit by using a so-called "summed fit" described in detail in Ref. [20]. Since the total lengths of the three runs were different, the summed analysis was performed on the individuals runs and the half-life was taken as the weighted average of the three results. In this summed analysis, the data were corrected for dead time [20]. The number of counts in each of the 250 bins of a given sample was adjusted for dead-time losses and these corrected counts were then added for all the samples. It should be noted that the initial count rate was sufficiently low that the initial dead time was, on average, lower than 2%.

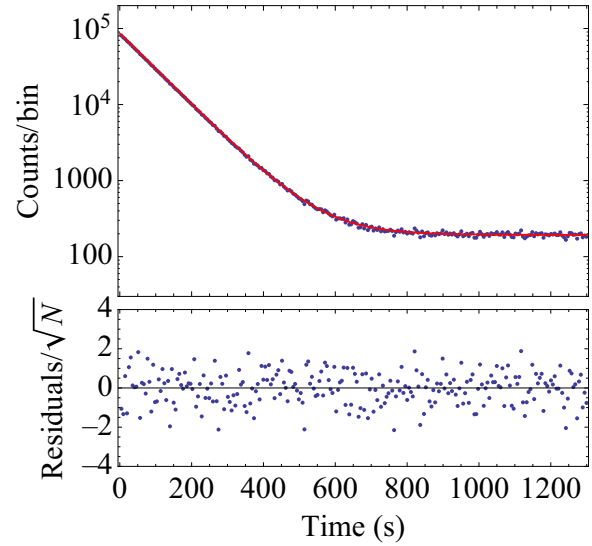

FIG. 3. Summed β-decay curves of all 18 samples of the third run together with the fitted curve including the observed ^{15}O contamination. Below are the residuals of the fit divided by the square root of the number of ions in a given bin N. Each bin is 5.2 s wide.

The decay curves were fit while accounting for the presence of ^{15}O contamination. This was done by using

$$r(t) = r_0(e^{-(\ln 2)t/t_1} + Re^{-(\ln 2)t/t_2}) + b \qquad (2)$$

for the observed decay rate. Here $R = 2.4\,(6) \times 10^{-3}$ is the ^{15}O-to-^{17}F contamination ratio measured before the first run and $t_2 = 122.24\,(27)$ s is the ^{15}O half-life from the literature [11].

Because the data collected in a counting experiment are a series of independent, discrete events, common least-square fitting methods, which assume Gaussian statistics, cannot be used [21,22]. Therefore, a maximum-likelihood-type fitting was used instead. The Poisson maximum likelihood was approached by iteratively performing least-square fittings [20,23] using a Levenberg–Marquardt algorithm. The iteration was stopped once variations of less than 0.01% in all of the fit parameters were observed [20]. A cross-check was performed by using a second common approach (see Ref. [24] for details), which involves fitting by minimizing a χ^2 value derived from Poisson statistics [22]. This yielded the same results. Finally, the fitting algorithms were tested by using artificially generated data.

Figure 3 shows the sum of the dead-time-corrected data for run 3 with the corresponding fit and normalized residuals. The reduced $\chi^2 = 0.68$ and the statistical spread of the residuals about a mean of -0.014 and a standard deviation of 0.83 suggest the absence of time-dependent systematic effects, such as non-negligible contamination or an improper accounting for dead time.

Table II gives the values of the fit parameters obtained for the summed fits of the three runs. Excellent consistency for the background and half-life values was obtained. In fact, all three half-lives agree within their uncertainties, leading to a Birge ratio of 0.62 (28). As a consistency check, a sum fit with the contamination ratio left floating also was performed. As seen

TABLE II. Fitting parameters from the summed fit of the three ^{17}F runs. The last row gives the weighted average of the above half-lives.

Run	r_0 (s^{-1})	b (s^{-1})	$t_{1/2}$ (s)
1	1018.2(6)	2.00(4)	64.424(39)
2	937.6(15)	2.08(5)	64.375(87)
3	888.9(11)	2.06(1)	64.366(60)
Mean			64.402(31)

in Fig. 4, this led to statistically distributed half-life values about the results from the fit with fixed R, with the measured ratio and average half-life agreeing within uncertainties. This consistency and the average of the fit contamination ratios, $R_{\text{float}} = 3.6\,(14) \times 10^{-3}$, verifies the estimated contamination ratio.

The accuracy of the fitting algorithm was then tested against a Monte Carlo simulated data set. Three data sets with parameters used in the experiment and the fitted values from Table II were generated. The same fitting algorithm used to fit the experimental data was used to fit the artificial data, and the results are given in Fig. 4. All three fit values agree within uncertainties with the half-life used to generate the hypothetical data. To verify that the differences are really of a statistical nature, the third data set was regenerated with $N_{\text{sample}} = 200$. The resulting $t_{1/2,\text{MC}} = 64.386\,(18)$ s is in very good agreement with the given half-life.

C. Uncertainty estimation

Various sources of uncertainties in the measurement and fitting were investigated. These sources of uncertainty include: the estimated contamination ratio, the uncertainty in the contaminant half-life, the uncertainty in the dead-time determination, the presence of other contaminants, and possible clock errors.

1. Contamination-related uncertainty

As discussed in the previous section, the summed fits with a free-floating contamination ratio validated both the estimated contamination ratio and the half-life as obtained using the measured contamination ratio. Nevertheless, the effect of the uncertainty of R on the half-life was investigated by performing summed fits with $R = 1.8 \times 10^{-3}$ and 3.0×10^{-3} for all three runs. Half of the difference in the weighted average of the half-lives was then taken as the uncertainty due to the contamination ratio estimation, resulting in an uncertainty of 28 ms.

Similarly, the uncertainty in the literature value of the ^{15}O half-life will also induce an uncertainty in the ^{17}F half-life. This effect was quantified by performing summed fits with $t_2 = 121.97$ s and 122.51 s for all three runs. Half the difference in the weighted half-lives was taken as the error due to the uncertainty on the ^{15}O half-life. It was found that this introduced a negligible uncertainty of 0.5 ms.

Finally, the presence of contamination that was not accounted for, as well as possible mis-evaluation of the dead-time, were investigated. This was done by removing the leading bins one by one and performing a summed half-life fit on the remaining bins, for each of the three runs, with $R = 2.4 \times 10^{-3}$. As indicated in Fig. 5, no time-dependent systematic trends are apparent. It should be noted that the data points in Fig. 5 are highly correlated because they are all based on the same data. Hence such correlation could result in the apparent oscillatory behavior of the centroid (although within the one standard deviation uncertainty of each point). Such oscillations could be seen in previous half-life measurements [24].

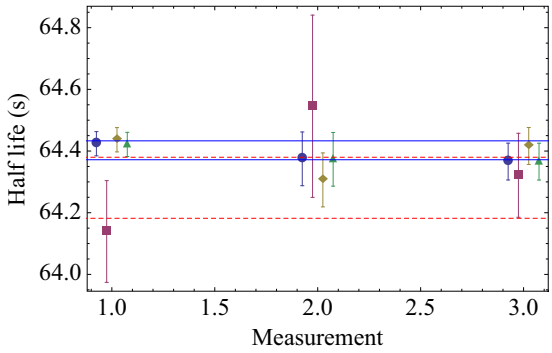

FIG. 4. Circles show half-lives obtained from a summed fit of the experimental data with $R = 2.4 \times 10^{-3}$. Squares show same as circles but with R left as a floating parameter. Diamonds show half-lives obtained from a summed fit of the Monte Carlo simulated data with $R = 2.4 \times 10^{-3}$. Triangles show the weighted average of the half-lives obtained from a sample-by-sample fit of the experimental data with $R = 2.4 \times 10^{-3}$. The two solid lines represent the one standard deviation error band for the weighted average of the summed fit with $R = 2.4 \times 10^{-3}$. The two dashed lines represent the one standard deviation error band for the weighted average of the summed fit with R left as a floating parameter.

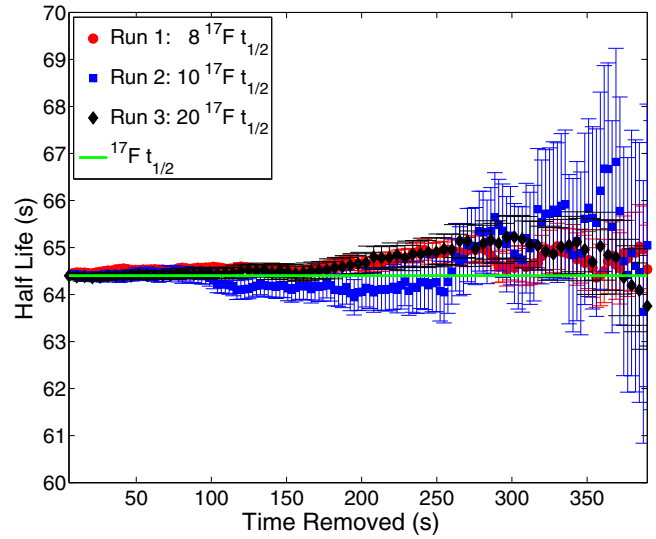

FIG. 5. Fitted half-lives for the summed data with the ^{15}O contamination ratio $R = 2.4 \times 10^{-3}$ as a function of the time removed at the beginning of the sample. Up to six half-lives were removed.

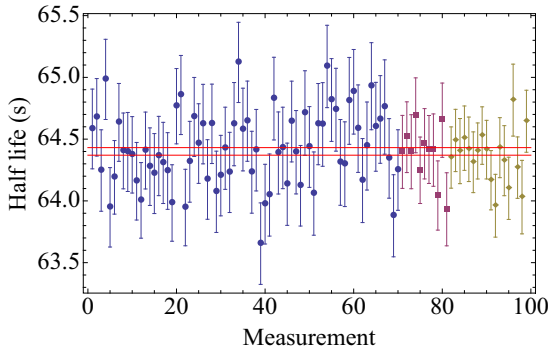

FIG. 6. Half-life results from the fitting of all individual samples. Circles indicate the first run, squares the second run, and diamonds the third run. The two red lines indicate the uncertainty on the weighted average on the half-life of all samples.

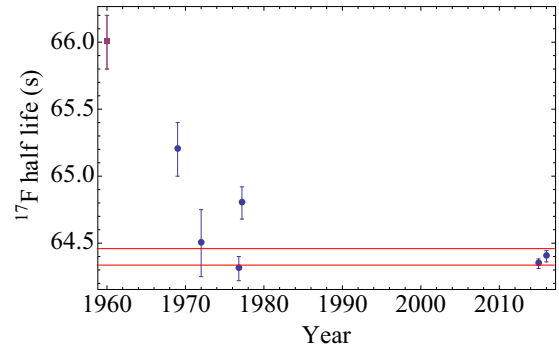

FIG. 7. Most recent ^{17}F half-lives [12–14,16,17,25] considered in the evaluation. Blue circles show half-lives used in the average. The 1960 value [25] was rejected due to possible unaccounted-for contamination. The scaled uncertainty on the overall ^{17}F half-life of 64.398 (56) s is represented by the red band.

2. *Other systematic effects*

The uncertainty in the determination of the dead time $\tau = 24.3\,(2)$ μs will also affect the ^{17}F half-life. Hence, similarly as done in the previous section, summed fits with $\tau = 23.9$ and $\tau = 24.5$ μs were performed for all three runs. Half of the weighted average of the half-life for the two cases was taken as the systematic uncertainty. The resulting value, 3.6 ms, was added in quadrature to the other systematic uncertainties.

To search for additional systematic errors (from effects that may vary with time, or from one run to another), as previously discussed, we fit each sample individually with a dead-time correction applied to the data. Figure 6 shows the half-life obtained from the 99 samples taken during the experiment. The half-life obtained from the weighted average of all samples is 64.401 (31) s, with a Birge ratio of 0.89 (5). Having a Birge ratio close to one indicates that the spread in the data is statistical in nature. Furthermore, this value is in excellent agreement with the half-life obtained from the summed fits.

Table III summarizes the various sources of uncertainties. The statistical uncertainty on the half-life is 31 ms, while the systematic uncertainty, primarily coming from the contamination ratio estimate, is evaluated to be 28 ms. Adding the statistical and systematic uncertainties in quadrature yields a ^{17}F half-life of 64.402 (42) s when a summed fit is used.

IV. ^{17}F HALF-LIFE

The new ^{17}F half-life measurement of 64.402 (42) s is in good agreement with the half-life value of 64.347 (35) s recently published by the GANIL group [12]. It is also lower than the first result [15], published by the same group, which had a larger uncertainty. Using our new ^{17}F half-life we performed an evaluation of all the published half-lives. Following the procedure of the Particle Data Group [26], measurements without reported error were not considered. Then, as done in previous half-life evaluations [3,11] we kept only the results that will influence the final half-life, i.e., only the results with a reported uncertainty that is smaller than ten times the uncertainty on the most precise measurement were considered. Most of the measurements not considered are pre-1960 (see Ref. [25] for a compilation of these measurements) and present systematically high values that cluster around 66 s. The larger half-life is most likely due to the presence of an unaccounted contaminant with a longer half-life in large-enough amount to affect the half-life, such as ^{15}O [11].

Figure 7 shows the sufficiently precise half-lives considered in the evaluation. The 1960 measurement from [25] deviates from the average half-life by 8σ. Upon close inspection, the article does not mention the presence of ^{15}O contamination. Furthermore, the 1969 measurement [13], which reported a lower half-life and used the same reaction and target (SiO_2) to produce ^{17}F, did observe the presence of ^{18}F and ^{30}P (2.498 minutes) from the ^{29}Si(d,n) reaction on the 4.7% abundant ^{29}Si. Hence, for these reasons, we did not include the 1960 measurement in our averaging. The 1969 measurement, which deviates from the average half-life by 4σ, was included in the average value since there were no obvious reasons to exclude it.

The weighted average of all results yields a half-life of 64.398 (25) s. The Birge ratio of the world data is 2.3 with the new measurement. Using the practices from the Particle Data Group [26] and scaling the uncertainty by the Birge ratio gives a ^{17}F half-life value of 64.398 (61) s. This new world average is shown by the red band in Fig. 7, together with the result from this work and previous half-life experiments.

The ^{17}F half-life is one of two experimental quantities needed to calculate the ft value of the $T = 1/2$ mixed transition. Since its last evaluation [11], another required quantity, the Q value, changed slightly to 2760.47 (25) keV [27]. Table IV shows the new f_v value, calculated by using the

TABLE III. Various sources of errors on the ^{17}F half-life.

Source	Uncertainty (ms)
Statistical	31
Contamination	28
^{15}O half-life	0.5
Dead time	3.6
Total	42

TABLE IV. Values for various parameters of relevance for determining V_{ud} from the ^{17}F mirror transition. The Q_{EC} value under "This work" is from the latest atomic mass evaluation [27].

Parameter	This work	Ref. [11]
Q_{EC}	2760.47(25) keV	2760.51(27) keV
f_v	35.208(22)	35.217(24)
$t_{1/2}$	64.398(61) s	64.61(17) s
$f_v t$	2270.7(26) s	2278.6(61) s
$\mathcal{F}t^{\text{mirror}}$	2292.4(27) s	2300.4(62) s
ρ	−1.2854(25)	−1.2815(35)
a_{SM}	0.1694(12)	0.1713(17)
A_{SM}	0.99719(13)	0.99739(18)
B_{SM}	0.64121(65)	0.64222(92)

parametrization from Ref. [28]. Then, using the new half-life, the electron capture fraction $P_{EC} = 0.147$, the theoretical corrections $\delta'_R = 1.587\,(10)$, and $\delta_C^V - \delta_{NS}^V = 0.62\,(3)$ from Ref. [11], we calculated a new $\mathcal{F}t^{\text{mirror}}$ value. By using this $\mathcal{F}t^{\text{mirror}}$ value, we can extract a value for the mixing ratio ρ using [11]

$$\mathcal{F}t^{\text{mirror}} = \frac{2\mathcal{F}t^{0^+\to 0^+}}{1 + \frac{f_A}{f_V}\rho^2}, \tag{3}$$

where $\mathcal{F}t^{0^+\to 0^+} = 3072.27\,(62)$ s is the average value for the 14 most precisely known pure Fermi $0^+ \to 0^+$ superallowed transitions and f_A is the axial-vector part of the statistical rate function, calculated by using the parametrization from Ref. [28]. By using this value for ρ we can calculate the measurable parameters a_{SM}, A_{SM}, and B_{SM} assuming that the ^{17}F mirror transition obeys the Standard Model. The only existing measurement of a correlation parameter is the measurement of $A_\beta = 0.960\,(82)$ from Ref. [29]. While this value agrees with our prediction in Table IV, it is found that ρ varies very weakly with A_β, leading to a large uncertainty in ρ. Hence, a measurement of the correlation parameter $a_{\beta\nu}$ would be more appropriate to extract ρ and compute V_{ud}.

V. OUTLOOK

With a relative uncertainty of 9.5×10^{-4}, the uncertainty of the world-average value of the half-life of ^{17}F is still greater than the relative uncertainty (6.2×10^{-4}) of the other precisely known quantity, the f_V value. This stems from the large $\chi^2 = 31$ of the current measurements of half-lives. More precision measurements with different systematics are needed to remedy the situation. Finally, the inclusion of ^{17}F for testing the conserved-vector-current hypothesis and for the extraction of the V_{ud} matrix element will require the measurement of the mixing ratio ρ. A dedicated Paul trap is currently being planned to perform such a measurement at the University of Notre Dame Nuclear Science Laboratory [30].

ACKNOWLEDGMENTS

We would like to thank O. Naviliat–Cuncic, J. C. Hardy, G. Ball, and J. Görres for fruitful discussions as well as X. Tang and B. Bucher for the fabrication of the β counter. This work was supported by the National Science Foundation (NSF) Grants No. PHY-1419765 and No. PHY-1401343.

[1] K. Blaum, J. Dilling, and W. Nörtershüser, Phys. Scr. **T152**, 014017 (2013).
[2] N. Severijns and O. Naviliat-Cuncic, Annu. Rev. Nucl. Part. Sci. **61**, 23 (2011).
[3] J. C. Hardy and I. S. Towner, Phys. Rev. C **91**, 025501 (2015).
[4] S. L. Glashow, Nucl. Phys. **22**, 579 (1961).
[5] I. S. Towner and J. C. Hardy, Rep. Prog. Phys. **73**, 046301 (2010).
[6] G. Savard, F. Buchinger, J. A. Clark, J. E. Crawford, S. Gulick, J. C. Hardy, A. A. Hecht, J. K. P. Lee, A. F. Levand, N. D. Scielzo, H. Sharma, K. S. Sharma, I. Tanihata, A. C. C. Villari, and Y. Wang, Phys. Rev. Lett. **95**, 102501 (2005).
[7] O. Naviliat-Cuncic and N. Severijns, Phys. Rev. Lett. **102**, 142302 (2009).
[8] G. Ban, D. Durand, X. Fléchard, E. Liénard, and O. Naviliat-Cuncic, Ann. Phys. (Berlin, Ger.) **525**, 576 (2013).
[9] N. Severijns, G. Neyens, and M. Bissell, CERN-INTC-2013-013/INTC-O-017, Section 2.2.3 (2013).
[10] J. C. Hardy and I. S. Towner, J. Phys. G **41**, 114004 (2014).
[11] N. Severijns, M. Tandecki, T. Phalet, and I. S. Towner, Phys. Rev. C **78**, 055501 (2008).
[12] J. Grinyer, G. F. Grinyer, M. Babo, H. Bouzomita, P. Chauveau, P. Delahaye, M. Dubois, R. Frigot, P. Jardin, C. Leboucher, L. Maunoury, C. Seiffert, J. C. Thomas, and E. Traykov, Phys. Rev. C **92**, 045503 (2015).
[13] K. Wohllenben and E. Schuster, Radiochimica Acta. **12**, 75 (1969).
[14] D. E. Alburger, Phys. Rev. C **16**, 889(R) (1977).
[15] G. F. Grinyer *et al.*, Nucl. Instrum. Methods Phys. Res., Sect. A **741**, 18 (2014).
[16] D. E. Alburger and D. H. Wilkinson, Phys. Rev. C **6**, 2019 (1972).
[17] G. Azuelos, J. E. Kitching, and K. Ramavataram, Phys. Rev. C **15**, 1847 (1977).
[18] F. D. Becchetti, M. Y. Lee, T. W. O'Donnell, D. A. Roberts, J. J. Kolata, L. O. Lamm, G. Rogachev, V. Guimaräes, P. A. DeYoung, and S. Vincent, Nucl. Instrum. Methods Phys. Res., Sect. A **505**, 377 (2003).
[19] A. P. Baerg, Int. J. Appl. Radiat. Isot. **24**, 401 (1973).
[20] V. T Koslowsky, E. Hagberg, J. C. Hardy, G. Savard, H. Schmeing, K. S. Sharma, and X. J. Sun, Nucl. Instrum. Methods Phys. Res., Sect. A **401**, 289 (1997).
[21] D. C. Robinson, Nucl. Instrum. Methods **79**, 65 (1970).
[22] S. Baker and R. D. Cousins, Nucl. Instrum. Methods Phys. Res. **221**, 437 (1984).
[23] J. W. Fowler, J. Low Temp. Phys. **176**, 414 (2014).
[24] G. F. Grinyer, C. E. Svensson, C. Andreoiu, A. N. Andreyev, R. A. E. Austin, G. C. Ball, R. S. Chakrawarthy, P. Finlay, P. E. Garrett, G. Hackman, J. C. Hardy, B. Hyland, V. E. Iacob, K. A. Koopmans, W. D. Kulp, J. R. Leslie, J. A. Macdonald,

A. C. Morton, W. E. Ormand, C. J. Osborne, C. J. Pearson, A. A. Phillips, F. Sarazin, M. A. Schumaker, H. C. Scraggs, J. Schwarzenberg, M. B. Smith, J. J. Valiente-Dobon, J. C. Waddington, J. L. Wood, and E. F. Zganjar, Phys. Rev. C **71**, 044309 (2005).
[25] V. J. Jänecke, Z. Naturforschg **15 a**, 593 (1960).
[26] J. Beringer *et al.*, Phys. Rev. D **86**, 010001 (2012).
[27] G. Audi, F. G. Kondev, M. Wang, B. Pfeiffer, X. Sun, J. Blachot, and M. MacCormick, Chin. Phys. C **36**, 1157 (2012).
[28] I. S. Towner and J. C. Hardy, Phys. Rev. C **91**, 015501 (2015).
[29] N. Severijns, J. Wouters, J. Vanhaverbeke, and L. Vanneste, Phys. Rev. Lett. **63**, 1050 (1989).
[30] M. Brodeur, J. Kelly, J. Long, C. Nicoloff, and B. Schultz, Nucl. Instrum. Methods Phys. Res., Sect. B (to be published).